

# Hydration of Tetraphenylphosphonium and Tetraphenylborate Ions by Dielectric Relaxation Spectroscopy

Wolfgang Wachter and Richard Buchner\*

*Institut für Physikalische und Theoretische Chemie, Universität Regensburg, D-93040 Regensburg, Germany*

Glenn Hefter\*

*Chemistry Department, Murdoch University, Murdoch, WA 6150, Australia*

*Received: December 9, 2005; In Final Form: January 18, 2006*

A systematic study of the dielectric relaxation spectra of aqueous solutions of NaBPh<sub>4</sub> and Ph<sub>4</sub>PCl has been made at solute concentrations of  $0.02 \leq c/M \leq 0.82$  and  $0.20$ , respectively, and over a wide range of frequencies ( $0.2 \leq \nu/\text{GHz} \leq 89$ ) at  $25^\circ\text{C}$ . The spectra were best described by a superposition of four Debye processes, consisting of a very small ion-pair contribution with an average relaxation time of about 300 ps, a “slow”-water relaxation at 17 ps, and two bulk-water relaxations at 8 ps and 0.25 ps, respectively. The slow-water process has been assigned to the presence of a sheath of water molecules surrounding BPh<sub>4</sub><sup>−</sup> and Ph<sub>4</sub>P<sup>+</sup>, whose structure has been enhanced by its proximity to the bulky hydrophobic phenyl rings. A structure-making effect on the remaining solvent water can also be observed at low concentrations. More importantly, BPh<sub>4</sub><sup>−</sup> and Ph<sub>4</sub>P<sup>+</sup> show almost identical hydration characteristics, which provides indirect support for the use of the tetraphenylphosphonium tetraphenylborate reference electrolyte assumption in deriving single-ion thermodynamic properties.

## 1. Introduction

Single-ion thermodynamic quantities are of importance in many areas of chemistry, including the interpretation of pH and the comparison of electrode potentials in different solvents.<sup>1–3</sup> They are also required for theoretical and modeling purposes since, at least for strong electrolytes, ions are the major species present in solution.<sup>1–6</sup>

However, as is well known, such quantities cannot be determined within the framework of thermodynamics.<sup>1–5</sup> This problem has been handled traditionally in two ways. The first is to adopt a purely arbitrary convention, as for example is done when defining the standard potential of the hydrogen electrode in aqueous solutions to be zero at all temperatures ( $E^\circ(\text{Pt}/\text{H}_2, \text{H}^+(\text{aq}))/\text{V} \equiv 0$ ).<sup>1–3</sup> This approach is satisfactory for the tabulation of data and for expressing relative values of the property of interest ( $E^\circ$  in this case), but provides little insight into the actual (often referred to as the “true” or “absolute”) values of such properties.<sup>1–5</sup> Such quantities can only be obtained by using an appropriate extrathermodynamic assumption, ETA (with “extra” having the sense of “outside of”). A great many such ETAs, depending on the particular property of interest, have been made over the years for the estimation of single ion thermodynamic quantities. These have been reviewed on many occasions.<sup>1–5</sup>

It must be noted that there is no a priori way in which the validity of such an ETA can be proven, except by comparison with other assumptions and by the chemical reasonableness of the values derived. Nevertheless, in recent years it has become generally accepted that the “least objectionable” of the current

ETAs are those that employ a reference electrolyte. This approach involves assuming that the measurable whole-electrolyte thermodynamic property  $Y$  of a carefully-selected salt ( $\text{RR}'$ ) can be apportioned in a well-defined way between its component cation ( $\text{R}^+$ ) and anion ( $\text{R}'^-$ ). The split is often taken to be equal, in which case

$$Y(\text{RR}') \equiv 2Y(\text{R}^+) \equiv 2Y(\text{R}'^-) \quad (1)$$

For some salts and/or properties, unequal splits have been proposed, but the idea remains the same. As with conventional scales, once a value of  $Y(\text{ion})$  has been established for one ion, those of all other ions can be obtained by simple additivity of measured whole salt properties (strictly, at infinite dilution).

The choice of the reference electrolyte  $\text{RR}'$  is critical. As discussed in detail elsewhere,<sup>1–5</sup> the requirements for the ideal reference electrolyte are, to some extent, mutually exclusive. The current preferred salts are either tetraphenylphosphonium tetraphenylborate ( $\text{Ph}_4\text{PBPh}_4$ , TPTB) or its arsenic analogue  $\text{Ph}_4\text{AsBPh}_4$  (TATB). These salts are favored because they contain ions that are large and have a low and highly delocalized charge. On the basis of the Born model<sup>7</sup> such ions should be only weakly solvated and, therefore, show minimal differences in their solvation characteristics. In addition, both cation and anion are of similar size (especially for TPTB) and chemical character, possessing a quasi-spherical surface of phenyl rings. These factors should minimize the inevitable differences associated with the solvation of opposite charges. Finally,  $\text{Ph}_4\text{M}^+$  and  $\text{BPh}_4^-$  are chemically stable in most solvents (unlike their alkyl counterparts) and are readily available commercially (unlike their perfluorinated analogues, which might show even weaker solvation effects).

\* To whom correspondence should be addressed: Richard.Buchner@chemie.uni-regensburg.de, g.hefter@murdoch.edu.au

The only significant disadvantage of TPTB or TATB as reference electrolytes is that they are too sparingly soluble in most solvents for their properties to be measured directly. Instead their values must be obtained by an appropriate combination of data measured for more soluble salts, for example

$$Y^\circ(\text{Ph}_4\text{PBPh}_4) = Y^\circ(\text{Ph}_4\text{PX}) + Y^\circ(\text{MBPh}_4) - Y^\circ(\text{MX}) \quad (2)$$

where typically  $\text{M}^+$  is an alkali metal ion and  $\text{X}^-$  is  $\text{ClO}_4^-$ ,  $\text{CF}_3\text{SO}_3^-$ , or a halide ion. The need for such measurements increases the cost and reduces the accuracy of the results.

The reliability of the TPTB/TATB assumption clearly depends on the similarity of the interactions of the solvent with the cation and anion of the reference electrolyte. As already noted, for thermodynamic quantities this cannot be assessed directly; nevertheless, the similarity of the ion-solvent interactions can be probed by other techniques. Surprisingly few such studies have been made. Perhaps the most significant to date has been the multinuclear NMR investigation by Popov et al.<sup>8</sup> These authors showed that the NMR resonance frequencies of the carbon and hydrogen atoms in  $\text{Ph}_4\text{As}^+$ ,  $\text{Ph}_4\text{P}^+$ , and  $\text{BPh}_4^-$  differ and that these differences are solvent-dependent. They concluded that the TPTB/TATB assumption has to be used cautiously. However, although the work of Popov et al. shows that the NMR shifts between the cation and anion differ, it is not clear how to quantify them in thermodynamic terms, say with respect to solvation strength. Measurements using other techniques would be useful to shed light on the solvation characteristics of  $\text{Ph}_4\text{M}^+$  and  $\text{BPh}_4^-$ .

Dielectric relaxation spectroscopy (DRS)<sup>9,10</sup> is a powerful technique for the study of ion-solvent interactions. DRS measures the response of a sample to an applied electromagnetic field, as a function of the field frequency,  $\nu$ , in the microwave region. The complex permittivity spectra  $\hat{\epsilon}(\nu) = \epsilon'(\nu) - i\epsilon''(\nu)$  so obtained can provide unique insights into the nature and dynamics of electrolyte solutions.<sup>6,11–13</sup> To our knowledge no DRS study of aqueous solutions containing  $\text{BPh}_4^-$  or  $\text{Ph}_4\text{P}^+$  has been made. Accordingly, the present paper describes a systematic investigation of the dielectric spectra of aqueous solutions of  $\text{NaBPh}_4$  and  $\text{Ph}_4\text{PCl}$  as representative salts containing these ions, with a view to comparing their hydration behaviour.

## 2. Experimental Section

Solutions were prepared gravimetrically without buoyancy corrections; however, for data-processing purposes, all concentrations are expressed in M, (mol solute)/(L solution). Densities required for the interconversion were determined using a vibrating-tube densimeter (Anton Paar DMA 60) at  $(25.0 \pm 0.005)^\circ\text{C}$  with an accuracy (NIST-traceable) of  $\pm 0.05^\circ\text{C}$ . The concentration range of  $0.02 \leq c/\text{M} \leq 0.82$  used for  $\text{NaBPh}_4(\text{aq})$  was limited only by the detectability of an observed effect (at low concentrations) and of the conductivity contribution (at high concentrations, see below). Owing to its high cost, measurements on  $\text{Ph}_4\text{PCl}(\text{aq})$  had to be limited to  $c \leq 0.20$  M. All salts were dried under high vacuum ( $\sim 10^{-5}$  bar) for at least 48 h using  $\text{P}_2\text{O}_5$  (Sicapent, Merck) as a desiccant:  $\text{NaBPh}_4$  (Merck, Pro Analysis, > 99.5 % purity) at  $20^\circ\text{C}$  and  $\text{Ph}_4\text{PCl}$  (Merck, zur Synthese, 98.4 %) at  $30^\circ\text{C}$ .

Dielectric spectra were recorded at  $\nu_{\min} \leq \nu/\text{GHz} \leq 20$  at Murdoch University using a Hewlett-Packard model 85070M dielectric probe system based on a HP 8720D vector network analyzer (VNA), as described previously.<sup>14</sup> Temperature was controlled by a Hetofrig (Denmark) circulator-thermostat to

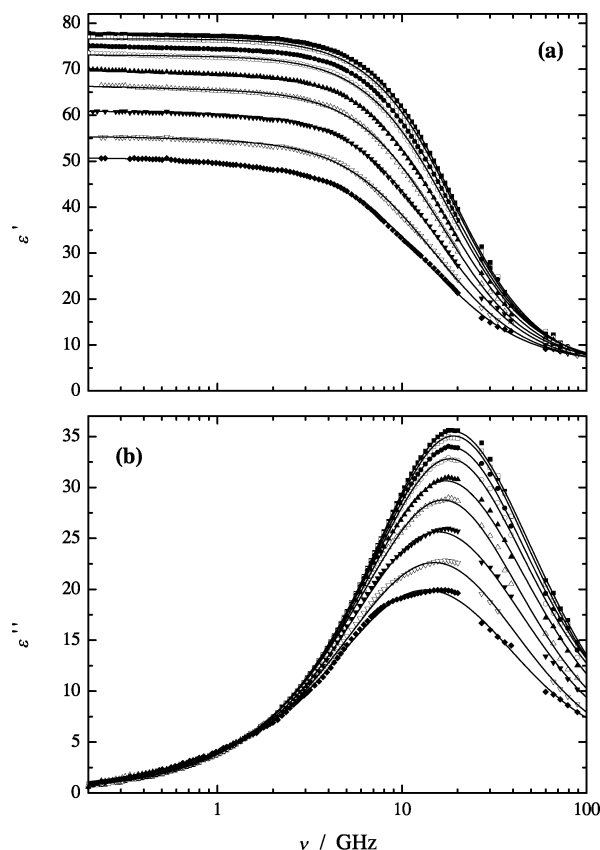


**Figure 1.** Dielectric permittivity (a) and loss (b) curves for  $\text{NaBPh}_4(\text{aq})$  at  $25^\circ\text{C}$  and concentrations  $c/\text{M} = 0.03, 0.05, 0.10, 0.15, 0.25, 0.35, 0.50, 0.67$ , and  $0.82$  (top to bottom).

$\pm 0.02^\circ\text{C}$ , with an accuracy of  $\pm 0.05^\circ\text{C}$ . The value of the minimum frequency of investigation,  $\nu_{\min}$ , was determined by the conductivity contribution to the loss spectrum. As such, it varied with concentration and salt but was typically in the range (0.2 to 0.4) GHz. All VNA spectra were recorded at least twice using independent calibrations with air, water, and mercury as the references. Higher frequency data were recorded at Regensburg using two interferometers: A-band ( $27 \leq \nu/\text{GHz} \leq 39$ ) and E-band ( $60 \leq \nu/\text{GHz} \leq 89$ ). The operation of these instruments is described in detail elsewhere.<sup>11,15</sup> Temperature control and accuracy were similar to those at Murdoch. Typical spectra and the corresponding fits are shown in Figures 1 and 2. All fitting parameters are summarized in Table 1.

## 3. Data Analysis

For an electrolyte solution of conductivity  $\kappa$ , DRS determines the relative dielectric permittivity,  $\epsilon'(\nu)$ , and the total loss,  $\eta''(\nu)$ , which is related to the dielectric loss  $\epsilon''(\nu)$

$$\eta''(\nu) = \epsilon''(\nu) + \kappa/(2\pi\nu\epsilon_0) \quad (3)$$

where  $\epsilon_0$  is the permittivity of free space. To obtain  $\epsilon''(\nu)$ , each VNA spectrum was analyzed separately to determine the slightly calibration-dependent effective conductivity at each concentration. As shown previously,<sup>16</sup>  $\kappa$  was obtained by fitting the experimental total loss curve to eq 3. The resulting  $\kappa$  values are generally 1–2 % smaller than conventional (low frequency) conductivity data<sup>17</sup> with slightly larger deviations at high electrolyte concentrations. Provided the  $\kappa$  values obtained in this way were sufficiently reproducible ( $\pm 2\%$  for at least two measurements) the averaged VNA spectra were combined with interferometer data. As can be seen from Figures 1 and 2 there

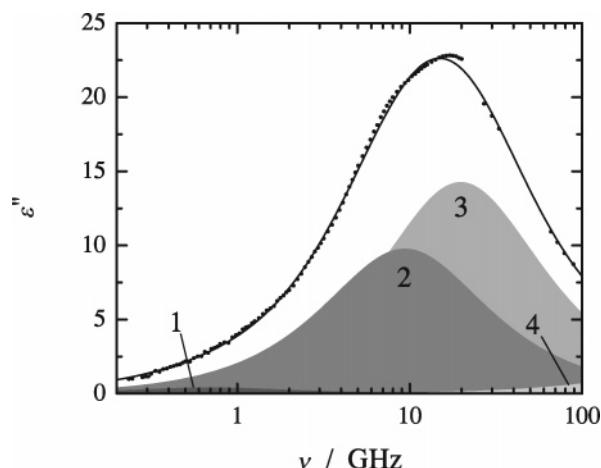


**Figure 2.** Dielectric loss curve of 0.67 M NaBPh<sub>4</sub>(aq) at 25 °C, showing the contributions of the four Debye processes (4D model, eq 4).

**TABLE 1: Conductivities,  $\kappa$ , and Parameters of the 4D/3D Model, eq 4: Limiting Permittivities  $\epsilon_1, \epsilon_2, \epsilon_3, \epsilon_4$  &  $\epsilon_\infty$ , Relaxation Times  $\tau_1, \tau_2, \tau_3$  &  $\tau_4$ , and Reduced Error Function,  $\chi^2_r$ , of NaBPh<sub>4</sub>(aq) & Ph<sub>4</sub>PCl(aq) at Concentration  $c$  and 25 °C<sup>a,b</sup>**

$c$	$\kappa$	$\epsilon_1$	$\tau_1$	$\epsilon_2$	$\tau_2$	$\epsilon_3$	$\tau_3$	$\epsilon_4$	$\tau_4$	$\epsilon_\infty$	$\chi^2_r$
NaBPh <sub>4</sub> (aq)											
0.0257	0.152			77.5	17F	75.4	8.23	6.00	0.5F	4.06	0.0583
0.0507	0.292			76.6	17F	72.6	8.17	5.82	0.5F	4.55	0.0535
0.101	0.542			74.7	17F	69.9	8.32	6.28	0.5F	2.91	0.0562
0.149	0.756	73.2	384	72.9	17F	66.7	8.41	6.53	0.5F	2.54	0.0488
0.250	1.14	69.8	365	69.2	17F	61.0	8.57	6.65	0.5F	1.91	0.0505
0.351	1.45	66.5	403	65.6	17F	54.5	8.66	6.53	0.5F	4.14	0.0590
0.501	1.78	60.9	347	60.3	17F	43.7	8.28	6.53	0.5F	2.82	0.0538
0.666	2.04	55.4	228	54.5	17F	35.0	8.05	6.42	0.5F	4.03	0.0409
0.824	2.12	50.8	207	49.4	17F	26.3	7.53	6.76	0.5F	2.33	0.0480
Ph <sub>4</sub> PCl(aq)											
0.0252	0.212			77.4	17F	78.0	8.51	6.19	0.5F	4.35	0.0817
0.0500	0.391			76.7	17F	75.2	8.47	5.90	0.5F	6.05	0.0559
0.0747	0.561			76.0	17F	72.0	8.40	6.12	0.5F	3.71	0.0778
0.100	0.719			75.1	17F	69.9	8.38	5.78	0.5F	5.35	0.0990
0.150	0.990	74.1	232	73.2	17F	69.0	8.69	6.48	0.5F	2.72	0.0695
0.200	1.25	72.6	236	71.4	17F	65.2	8.75	6.40	0.5F	3.42	0.0836

<sup>a</sup> Parameter values followed by the letter F were not adjusted in the fitting procedure. <sup>b</sup> Units:  $c$  in M;  $\kappa$  in  $\Omega^{-1}\text{m}^{-1}$ ;  $\tau_1, \tau_2, \tau_3$ , and  $\tau_4$  in  $10^{-12}$  s.

is, in general, a good fit between the low and high frequency data although, as is usually observed for electrolyte solutions, the noise increases with increasing solute concentration (conductivity).<sup>14,16</sup>

The combined  $\hat{\epsilon}(\nu)$  data were analyzed by simultaneously fitting the in-phase ( $\epsilon'(\nu)$ , see for example Figure 1a) and out-of-phase ( $\epsilon''(\nu)$ , Figure 1b) components to various relaxation models consisting of  $n$  distinguishable relaxation processes. It was found that the superposition of four Debye processes (a 4D model)

$$\hat{\epsilon}(\nu) = \epsilon_\infty + \frac{\epsilon_1 - \epsilon_2}{1 + (i2\pi\nu\tau_1)} + \frac{\epsilon_2 - \epsilon_3}{1 + (i2\pi\nu\tau_2)} + \frac{\epsilon_3 - \epsilon_4}{1 + (i2\pi\nu\tau_3)} + \frac{\epsilon_4 - \epsilon_\infty}{1 + (i2\pi\nu\tau_4)} \quad (4)$$

provided the best overall description of the dielectric data for the investigated solutions at  $c > 0.1\text{M}$ . At lower concentrations a 3D model (see below) was used. The fits did not support trial assumptions of more complicated band shapes, as for example

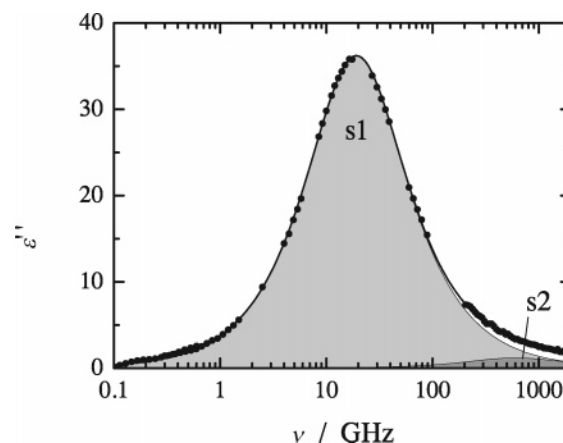


**Figure 3.** Broadband dielectric loss curve of water at 25 °C. Experimental data are described by a superposition of two Debye equations (2D model) with “s1” and “s2” denoting the contributions of the cooperative and the fast water relaxations, respectively.

described by the Havriliak–Negami equation,<sup>18</sup> for the individual relaxation processes.

In eq 4,  $\epsilon_\infty$  is the infinite-frequency permittivity and  $\tau_j$  the average relaxation time for the  $j$ th dispersion step ( $j = 1 \dots 4$ ). In principle  $\epsilon_\infty$  reflects only contributions from intramolecular polarizability. It can be obtained from either dielectric measurements at very high frequencies, or as an additional fitting parameter in the analysis of  $\hat{\epsilon}(\nu)$  data. Note that  $S_j = \epsilon_j - \epsilon_{j+1}$  is the amplitude (relaxation strength) of the  $j$ th dispersion step, and  $\epsilon \equiv \epsilon_1 = \epsilon_\infty + \sum S_j$  is the static (zero-frequency) permittivity of the sample.

Before discussing the results for the salt solutions in detail, it is useful to briefly review existing knowledge for water because its relaxation processes dominate the dielectric spectra of all of the solutions investigated here.

**3.1. Dielectric Spectrum of Water.** The dielectric spectrum for water at 25 °C over a wide range of frequencies is given in Figure 3; it is based on measurements in our laboratories and from other sources.<sup>19–22</sup> The observed spectrum is dominated by the process centred on 18 GHz ( $\tau_{s1} \approx 8$  ps), which is generally ascribed to the cooperative relaxation of bulk water molecules.<sup>20</sup> This process is the major feature of all of the present spectra. Interpretation of the minor faster process, which is barely detectable at  $\nu < 100$  GHz in pure water and is sometimes shifted to higher frequencies in salt solutions,<sup>20,22,23</sup> has long been controversial. Recent studies,<sup>24,25</sup> combining dielectric data in the THz region ( $500 \leq \nu/\text{GHz} \leq 5000$ ) at varying temperatures with far-IR spectroscopy, have shown that this small-amplitude feature is definitely a relaxation process, centred on 600 GHz ( $\tau_{s2} \approx 0.25$  ps), rather than one of the low energy intermolecular vibrations that occur at slightly higher frequencies.<sup>26</sup> Thus the pure water spectrum over the frequency range investigated here,  $\nu \leq 89$  GHz, is best described as a combination of two relaxation processes, with each  $\epsilon''(\nu)$  contribution having a Debye shape.

**3.2. Dielectric Spectra of the Salt Solutions.** As noted above, the superposition of four Debye equations (eq 4) gave the best description of the measured data. The lowest frequency process (of amplitude  $S_1 = S_{\text{IP}} = \epsilon_1 - \epsilon_2$ ) in the 4D model is solute-related and is most plausibly ascribed to the presence of very small amounts of ion pairs (IPs). The magnitude of the second process indicates that it is solvent-related and is most probably due to the presence of “slow” water molecules hydrating the large hydrophobic ions. The two higher-frequency processes are the water relaxations discussed above.

Due to the small ion-pair concentrations, the slowest process could not be resolved at  $c \lesssim 0.15\text{M}$  so that  $\epsilon_2$  of eq 4 becomes the static permittivity  $\epsilon$ , and the 4D fit reduces to a 3D fit. The fitting parameters for the combined 4D/3D model are given in Table 1.

As has been observed for the aqueous solutions of some sodium salts,<sup>27</sup> experimental data could also be described by a single Cole–Cole (CC) equation. However, the CC model, which describes a *symmetrically*-broadened process yielded significantly poorer results, even after allowing for the differing number of adjustable parameters. The reason why the CC model works at all for these solutions is because there are lower-frequency processes occurring that, when combined with the two bulk-water processes, produce a roughly symmetrical broadening of the dielectric spectrum. This model is, therefore, not physically realistic and so will not be considered further.

## 4. Results and Discussion

**4.1. Solute Relaxation and Ion Pairing.** The position and the small magnitude of the lowest-frequency process in the 4D model for the present solutions are consistent with the presence of small concentrations of  $\text{NaBPh}_4^0(\text{aq})$  or  $\text{Ph}_4\text{PCl}^0(\text{aq})$  ion pairs, as appropriate. Aggregates of same-charged ions, which have been claimed in the literature to exist, at least for  $\text{BPh}_4^-$ ,<sup>28</sup> do not possess a permanent dipole moment and thus will not be detected by DRS.

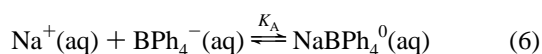
Since the  $\text{Ph}_4\text{PCl}$  solutions were investigated only at  $c \leq 0.2\text{M}$ , and as the ion-pair relaxation process could only be resolved for  $c \geq 0.15\text{M}$  (see above), a quantitative description of  $\text{Ph}_4\text{PCl}^0(\text{aq})$  ion-pair formation was not possible. However, for  $\text{NaBPh}_4$  solutions, realistic ion-pair concentrations,  $c_{\text{IP}}$ , could be derived in the concentration range  $0.15 \leq c/\text{M} \leq 0.82$  using the Cavell equation. For the present system, this can be written<sup>9,29</sup>

$$c_{\text{IP}} = \frac{3(\epsilon + (1 - \epsilon)A_{\text{IP}})}{\epsilon} \cdot \frac{k_{\text{B}}T\epsilon_0}{N_{\text{A}}} \cdot \frac{(1 - \alpha_{\text{IP}}f_{\text{IP}})^2}{\mu_{\text{IP}}^2} \cdot (\epsilon - \epsilon_2) \quad (5)$$

where  $\epsilon_2$  can be thought of as the permittivity of the solvent in the solutions. The subscript IP denotes an ion pair of dipole moment  $\mu_{\text{IP}}$  and polarizability  $\alpha_{\text{IP}}$ , along with a reaction field factor  $f_{\text{IP}}$  and shape factor  $A_{\text{IP}}$ , which can be calculated from the radii of the ions and of water as described previously.<sup>30</sup> Other symbols have their usual meanings<sup>31</sup> or have already been defined above.

To estimate the required ion-pair properties, an assumption must be made about the nature and geometry of the ion pair.<sup>30</sup> Taking into account the well established hydration shell of  $\text{Na}^+$  and the hydrophobic character of  $\text{BPh}_4^-$ , a solvent-shared ion pair (SIP) seems to be the most probable species. However, for comparison, calculations based on double-solvent-separated ion pairs (2SIPs) were also performed. Contact ion pairs (CIPs) are considered unlikely.

For the ion-pairing equilibrium



the association constant  $K_{\text{A}}$  is given by

$$K_{\text{A}} = \frac{c_{\text{IP}}}{(c - c_{\text{IP}})^2} = \frac{c_{\text{IP}}}{I^2} \quad (7)$$

as a function of the ionic strength  $I = \sum c_i z_i^2/2$  ( $= c - c_{\text{IP}}$  for this system), where  $z_i$  is the charge number of the ion  $i$ . A value

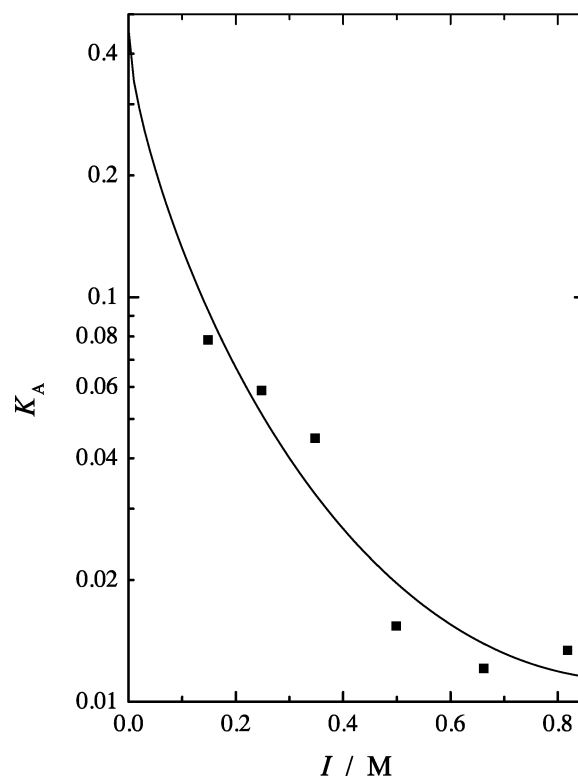


**Figure 4.** Ion association constant,  $K_{\text{A}}$ , as a function of the ionic strength,  $I$ , of  $\text{NaBPh}_4(\text{aq})$  at 25 °C (SIP model).

**TABLE 2: Experimental and Calculated<sup>a</sup> Rate Constants for the Formation,  $k_1$ , and Dissociation,  $k_{-1}$ , of Ion Pairs of  $\text{NaBPh}_4$  in Aqueous Solution at 25 °C, and Corresponding Association Constants,  $K_{\text{A}}^\circ$ , and Empirical Parameters  $B_{\text{K}}$ ,  $C_{\text{K}}$ <sup>b</sup>**

model	$k_1$	$k_1^{\text{calc}}$	$k_{-1}$	$k_{-1}^{\text{calc}}$	$K_{\text{A}}^\circ$	$B_{\text{K}}$	$C_{\text{K}}$
SIP	$1.8 \pm 0.4$	7.0	$4 \pm 15$	5.4	$0.5 \pm 1.9$	$-3.8 \pm 2.1$	$2.7 \pm 2.1$
2SIP	$0.8 \pm 0.2$	11	$2 \pm 17$	3.3	$0.3 \pm 1.9$	$-3.8 \pm 2.1$	$2.7 \pm 2.0$

<sup>a</sup> Via the Eigen theory.<sup>41,27</sup> <sup>b</sup> Units:  $k_1$  in  $10^9 \text{ s}^{-1}$ ,  $B_{\text{K}}$  in  $\text{M}^{-1}$ ;  $C_{\text{K}}$  in  $\text{M}^{-3/2}$ .

of the standard (infinite dilution) association constant,  $K_{\text{A}}^\circ$ , was derived by fitting the values of  $K_{\text{A}}$  to a Guggenheim-type equation<sup>32,33</sup> (Figure 4)

$$\log K_{\text{A}} = \log K_{\text{A}}^\circ - \frac{2A_{\text{DH}}|z_+z_-|\sqrt{I}}{1 + A_{\text{K}}\sqrt{I}} + B_{\text{K}}I + C_{\text{K}}I^{3/2} \quad (8)$$

where  $A_{\text{DH}}$  is the Debye–Hückel constant ( $0.5115 \text{ L}^{1/2}\text{mol}^{-1/2}$  for water at 25 °C), and  $X_{\text{K}}$  are adjustable parameters ( $A_{\text{K}}$  was fixed at  $1.00 \text{ M}^{-1/2}$  throughout).<sup>33</sup>

The  $K_{\text{A}}^\circ$ ,  $B_{\text{K}}$ , and  $C_{\text{K}}$  values obtained in this way for  $\text{NaBPh}_4^0(\text{aq})$ , assuming the formation of either SIPs or 2SIPs, are given in Table 2. Their similarity of the fitting parameters and their large uncertainties are typical of those observed for systems involving  $\text{Na}^+$  with other weakly-complexing anions.<sup>27</sup> The existence of weak ion pairing in aqueous solutions of  $\text{NaBPh}_4$  is supported by the conductivity measurements of Schiavo et al.,<sup>34</sup> who give  $K_{\text{A}}^\circ = 4.6$  for  $\text{NaBPh}_4(\text{aq})$ . This is somewhat higher than the present results but still in reasonable agreement given the weakness of the association and the approximations required in both techniques.

It should be emphasised that the quantitative detection of such weak complexes is not trivial. This level of ion pairing is at the limits of detection of the present DRS apparatus, and it may be



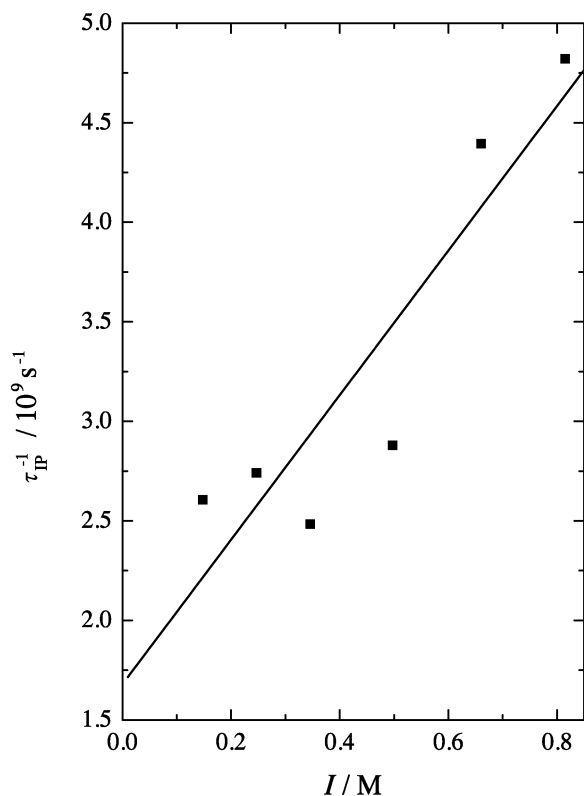


**Figure 5.** Ion-pair relaxation rate,  $\tau_{IP}^{-1}$ , as a function of the ionic strength,  $I$ , in NaBPh<sub>4</sub>(aq) solutions at 25 °C.

noted that both SIPs and 2SIPs are not usually detectable by the normally powerful UV–vis, NMR, or Raman spectroscopic techniques.<sup>35–37</sup> In this context it is unsurprising that the UV–vis study of Covington and Tait<sup>38</sup> did not detect ion pairs and so the use of their findings to postulate the existence of anion aggregates<sup>28</sup> is not reasonable. As already noted, since such aggregates would have a dipole moment of approximately zero, they cannot explain the present DRS observations, albeit their presence at high concentrations cannot be excluded.

**4.2. Ion-Pairing Kinetics.** The presence of a significant decrease in  $\tau_{IP}$  with increasing NaBPh<sub>4</sub> concentrations (see Table 1) is indicative of a kinetic contribution to the ion-pairing process. If a single-step process is assumed for equilibrium 6, which is reasonable in the present case as only one ion-pair process is detected, then the observable relaxation rate  $\tau_{IP}$  is given by<sup>39</sup>

$$\frac{1}{\tau_{IP}} = \frac{1}{\tau_{or}} + \frac{1}{\tau_{ch}} = \frac{1}{\tau_{or}} + k_{-1} + 2k_1(c - c_{IP}) \quad (9)$$

where  $\tau_{or}$  is the rotational correlation time of the ion pair, with  $k_1$  and  $k_{-1}$  being the rate constants for the formation and decay of the ion pair (cf. eq 6). A plot of  $\tau_{IP}^{-1}$  against the ionic strength  $I$  (Figure 5) yields  $k_1$  from the slope, while  $k_{-1}$  is given by  $k_1/K_A^\circ$ .<sup>39,40</sup> The results so obtained—especially for  $k_{-1}$  (Table 2)—are of the order of magnitude expected from the Eigen theory<sup>27,41</sup> for diffusion-controlled ion pairing, in accordance with the small association constant.

**4.3. Solvent Relaxation Processes.** As noted above, the dielectric spectrum of pure water is dominated by the process centred on 18 GHz (Figure 3), which is generally ascribed to the cooperative relaxation of bulk water molecules. In addition, there is a minor faster relaxation, centred on 600 GHz, which is associated with the reorientation of “free” water molecules into new hydrogen-bond configurations and small memory

effects associated with dielectric friction.<sup>25</sup> These two dispersion steps correspond to processes 3 and 4 in the dielectric spectra of the present solutions (Figures 1 and 2).

As process 4 represents water molecules rejoining the H-bonded water network, it is reasonable to combine it with process 3 to give an overall bulk-water amplitude of  $S_b = S_3 + S_4$ . Apparent solvent concentrations in the solutions,  $c_s^{\text{app}}$ , can then be calculated via the solvent-normalised Cavell equation<sup>29,42</sup>

$$c_s^{\text{app}}(c) = \frac{2\epsilon(c) + 1}{2\epsilon(0) + 1} \cdot \frac{\epsilon(0)}{\epsilon(c)} \cdot \frac{(1 - \alpha_s f_s(c))^2}{(1 - \alpha_s f_s(0))^2} \cdot \frac{c_s^\circ(0)}{S_b(0)} \cdot S_b(c) \quad (10)$$

where  $\alpha_s$  is the polarizability and  $f_s$  the reaction field factor of the solvent, and  $c_s^\circ$  is the analytical solvent concentration.

Application of eq 10 reveals that  $c_s^{\text{app}}(c)$  becomes significantly lower than  $c_s^\circ(c)$  with increasing electrolyte concentration,  $c$ . The large magnitude of these differences is explained most plausibly by assuming that process 2 is also due to solvent water. The average relaxation time for this process, which for fitting purposes was fixed at 17 ps for all solutions, is significantly longer than that of the major bulk water relaxation at 8 ps and is typical of a so-called *slow-water* process. Such processes have been observed previously for R<sub>4</sub>NX(aq),<sup>43</sup> for micellar systems<sup>44</sup> and for aqueous solutions of some sodium salts containing large carboxylate ions.<sup>45</sup> For R<sub>4</sub>NX(aq), slow water molecules are those that take part in hydrophobic hydration of the cations,<sup>43</sup> whereas for the carboxylates they are associated with the anions.<sup>45</sup> Thus, consistent with earlier literature speculations based on heat capacity measurements,<sup>28,46,47</sup> it seems reasonable to conclude that hydrophobic hydration of the tetraphenyl ions also occurs, which results in the formation of “slow” water in these solutions.

The general observation of a slow-water relaxation for hydrophobic solutes can be understood on the following grounds. According to the commonly-accepted scenario,<sup>25,48–50</sup> the cooperative dynamics of water are governed by the presence of “fifth neighbors”, i.e., by H<sub>2</sub>O molecules approaching, but not yet participating in a local H-bond configuration. Through their interactions with the H-bond network these “impurities”<sup>51</sup> can modify the energy of a bound water molecule and initiate the breaking of its H-bonds. Additionally, these fifth neighbors may act as new H-bond acceptors or donors when the released water molecule and its surroundings relax into a new equilibrium configuration. The increased number of H-bonds among the solvent molecules adjacent to a hydrophobic entity,<sup>43</sup> which results in slower dynamics of the primary hydration shell, is *not* a result of stronger H-bonds but merely a consequence of the shielding by the ions of those water molecules against the attack of fifth neighbours.

Analogous to eq 10, the solvent-normalized Cavell equation,

$$c_{\text{slow}}^{\text{app}}(c) = \frac{2\epsilon(c) + 1}{2\epsilon(0) + 1} \cdot \frac{\epsilon(0)}{\epsilon(c)} \cdot \frac{(1 - \alpha_s f_s(c))^2}{(1 - \alpha_s f_s(0))^2} \cdot \frac{c_s^\circ(0)}{S_2(0)} \cdot S_2(c) \quad (11)$$

then allows calculation of the apparent concentration of slow water,  $c_{\text{slow}}^{\text{app}}(c)$ , from which the number of slowly-relaxing water molecules per salt molecule,  $Z_{\text{slow}}$ , can be obtained:

$$Z_{\text{slow}} = \frac{c_{\text{slow}}^{\text{app}}(c)}{c} \quad (12)$$

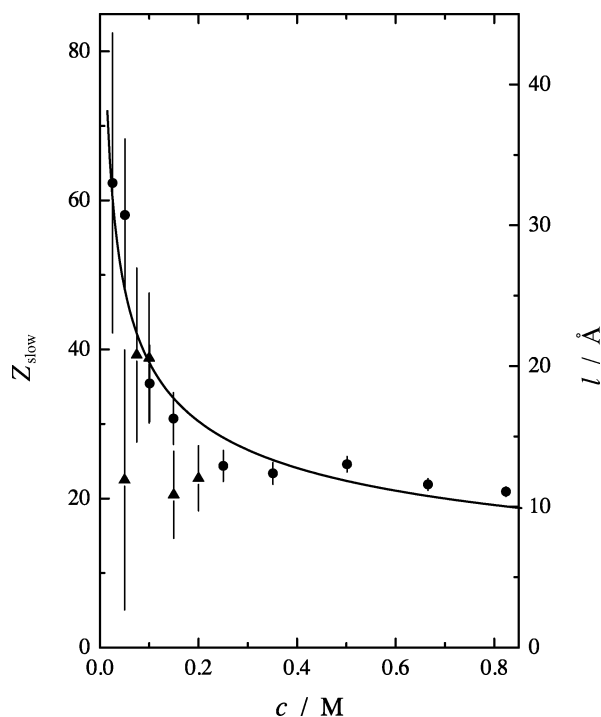


**Figure 6.** Concentration dependence of the hydrophobic hydration number  $Z_{\text{slow}}$  for NaBPh<sub>4</sub>(aq) (●) and Ph<sub>4</sub>PCl(aq) (▲) and of the average ionic distance  $l$  (line, right-hand scale) according to eq 13.

The  $Z_{\text{slow}}$  values calculated in this way for NaBPh<sub>4</sub>(aq) and Ph<sub>4</sub>PCl(aq) are shown in Figure 6.

Since aqueous solutions of typical inorganic salts containing sodium and chloride ions do not show any slow water process,<sup>27,52</sup> it is reasonable to interpret  $Z_{\text{slow}}$  for NaBPh<sub>4</sub>(aq) and Ph<sub>4</sub>PCl(aq) as a hydrophobic hydration number for BPh<sub>4</sub><sup>−</sup>(aq) and Ph<sub>4</sub>P<sup>+</sup>(aq), respectively. Although very large (Figure 6), the values of  $Z_{\text{slow}} \approx 60$  for the most dilute solutions are physically reasonable. Assuming the hydrated BPh<sub>4</sub><sup>−</sup> ion to be a sphere of radius ( $r_{\text{BPh}_4^-} + 2r_{\text{H}_2\text{O}}$ ), a surface area of 625 Å<sup>2</sup> and a hydrate shell volume of 1157 Å<sup>3</sup> are obtained with  $r_{\text{BPh}_4^-} = 4.21$  Å<sup>53</sup> and  $r_{\text{H}_2\text{O}} = 1.425$  Å.<sup>54</sup> If it is then assumed that the area occupied by one water molecule is  $4\pi r_{\text{H}_2\text{O}}^2$ , a total of 77 water molecules would be required to cover the surface of this sphere, ignoring packing effects. Alternatively, if the volume of a water molecule is taken as  $(4/3)\pi r_{\text{H}_2\text{O}}^3$ , the hydrate shell volume provides space for 95 water molecules, again ignoring packing effects. Similar values are obtained for Ph<sub>4</sub>P<sup>+</sup>. A more exact geometrical estimation of the volume required by the solvent molecules yields<sup>47</sup> a maximal value of 60 water molecules in the first hydration shell of BPh<sub>4</sub><sup>−</sup>.

For NaBPh<sub>4</sub> solutions,  $Z_{\text{slow}}$  decreases strongly with increasing solute concentration until it reaches a plateau value of  $\sim 23$  at  $c \geq 0.25$  M; results similar to these were obtained for Ph<sub>4</sub>PCl solutions although the values are rather scattered (Figure 6). It is noteworthy that the concentration dependence of  $Z_{\text{slow}}$  shows a pattern similar to that of the average ionic separation  $l$  in solution:

$$l = Ac^{-1/3} \quad (13)$$

with the parameter  $A$  having the value of  $9.40 \text{ Å mol}^{1/3}\text{L}^{-1/3}$  for 1:1 electrolytes.<sup>55</sup> Note that at  $\sim 0.35$  M, the average distance between the ions has already dropped to the sum of the radii of two hydrated BPh<sub>4</sub><sup>−</sup> ions.

This strong decrease of  $Z_{\text{slow}}$  with increasing solute concentration is characteristic of hydrophobic hydration<sup>43</sup> and probably

reflects the combination of three effects: (i) the clustering of BPh<sub>4</sub><sup>−</sup>/Ph<sub>4</sub>P<sup>+</sup> ions to minimize the exposed, energetically unfavorable, hydrophobic surface and to optimize water–water contacts; (ii) the breakdown of the hydration shells due to increasing ion–ion interactions; and (iii) the possible breakdown of the bulk-water structure (see below). Given the existence of a slow-water process involving a significant number of solvent molecules, it must be concluded that, at least for  $c \rightarrow 0$ , both BPh<sub>4</sub><sup>−</sup> and Ph<sub>4</sub>P<sup>+</sup> exert a structuring effect on the first hydration layer.

**4.4. Bulk-Water Relaxation Processes.** While Ph<sub>4</sub>P<sup>+</sup> is generally regarded in the literature as a structure maker,<sup>53,56,57</sup> the structure-making or -breaking characteristics of BPh<sub>4</sub><sup>−</sup> are controversial. For example, Millero<sup>58</sup> found that the temperature dependence of the partial molar expansibilities  $\partial E^\circ/\partial T$  of NaCl(aq) and NaBPh<sub>4</sub>(aq) have similar negative values and, following Hepler,<sup>59</sup> suggested BPh<sub>4</sub><sup>−</sup> is a structure breaker. Near-IR spectra<sup>60</sup> indicated that the interactions between water and NaBPh<sub>4</sub> are comparable with the interactions between water and the structure-breaking salts NaCl, NaBr, or NaI. Similarly, FTIR spectra<sup>61</sup> of HDO revealed a strong similarity between NaClO<sub>4</sub>, a well-known structure breaker,<sup>53</sup> and NaBPh<sub>4</sub>. However, as Joliet et al.<sup>60</sup> pointed out, IR spectra in aqueous solutions often reflect the superposition of several contributions so that similarities between different electrolytes may not be significant.

Coetzee and Sharpe<sup>62</sup> observed that addition of NaBPh<sub>4</sub> to water caused a high-field NMR shift of the H<sub>2</sub>O protons whereas Ph<sub>4</sub>PCl yielded a low-field shift; they tentatively concluded that BPh<sub>4</sub><sup>−</sup> might be structure-breaking and Ph<sub>4</sub>P<sup>+</sup> structure-making. However, this conclusion depends on the assumption used to separate the cation and anion contributions. Little justification was given for the assumption adopted,  $\delta^1\text{H}(\text{Et}_4\text{N}^+) = 0$ ,<sup>62</sup> which produced the distinction between BPh<sub>4</sub><sup>−</sup> and Ph<sub>4</sub>P<sup>+</sup>. Such an inference is also contradicted by the NMR rotational correlation times of water molecules,  $\tau_c$ , which show almost identical values of  $\tau_c(\text{BPh}_4^-) = 5.42$  ps and  $\tau_c(\text{Ph}_4\text{P}^+) = 5.11$  ps.<sup>56</sup> These values are consistent with an increased lifetime of the intermolecular bonds among the H<sub>2</sub>O molecules in the vicinity of the tetraphenyl ions ( $\tau_c = 2.51$  ps in pure water), thereby identifying them both as structure makers. A structure-making classification for BPh<sub>4</sub><sup>−</sup> is also supported by conductivity data,<sup>57</sup> which show that NaBPh<sub>4</sub> has a lower Walden product in water than in organic solvents (implying water structuring), and by calorimetric measurements.<sup>28,46,47</sup> It is also noteworthy that the empirical scale of structuring abilities proposed by Marcus,<sup>53,63</sup> based on entropy data, classifies both BPh<sub>4</sub><sup>−</sup> and Ph<sub>4</sub>As<sup>+</sup> as structure makers (no value was given for Ph<sub>4</sub>P<sup>+</sup>).

From this discussion, and that in section 4.3, it seems reasonable to classify both Ph<sub>4</sub>P<sup>+</sup> and BPh<sub>4</sub><sup>−</sup> as structure makers with respect to their primary hydration shell. A question then arises as to how far this influence on water structure extends into the bulk. It is possible that the conflicting literature views arise from an inappropriate comparison of methods that are specific to H<sub>2</sub>O in the immediate vicinity of the hydrophobic solute with those that average over all water configurations.

As already discussed, relaxation processes 3 and 4 are associated with bulk water. Analysis of  $S_b = S_3 + S_4$  and of the cooperative (bulk) relaxation time  $\tau_3$  should, therefore, shed some light on the effect of the ions beyond their primary hydration shell. As will be shown below, the present results reconcile the conflicting assignments of BPh<sub>4</sub><sup>−</sup> (or NaBPh<sub>4</sub>) as structure making or breaking.

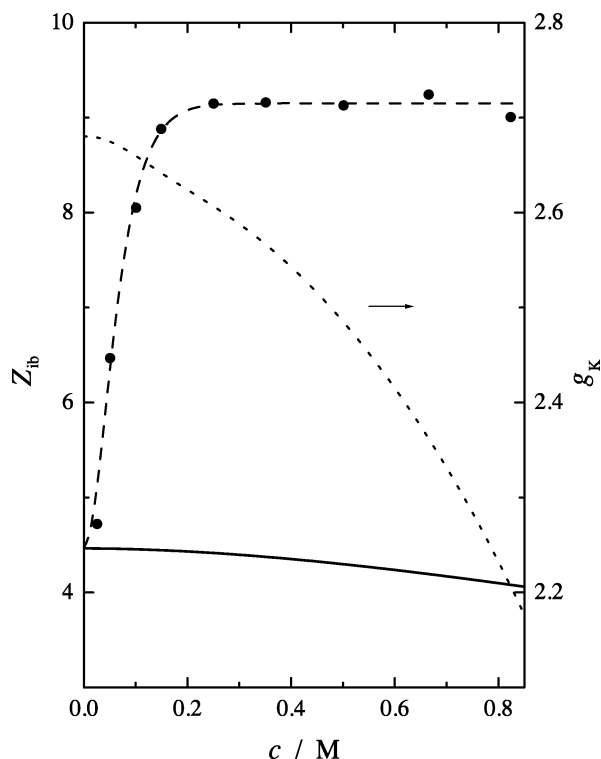


**Figure 7.** Concentration dependence of the effective hydration numbers,  $Z_{IB}$ , for NaBPh<sub>4</sub>(aq) (●, dashed line given only as a visual aid) and for Na<sup>+</sup> (solid line), and the Kirkwood factor  $g_K(c)$  (dotted line, right-hand scale).

Given that process 2 is also a water relaxation, an effective solvation number,  $Z_{IB}$ , which can be defined as the average number of solvent molecules irrotationally bound (IB) on the DRS timescale to one electrolyte ‘molecule’, can be calculated as

$$Z_{IB} = \frac{c_s^o - c_s^{app} - c_{slow}^{app}}{c} \quad (14)$$

The  $Z_{IB}$  values so obtained for NaBPh<sub>4</sub> solutions are given in Figure 7. The corresponding values for Ph<sub>4</sub>PCl(aq) were too scattered to justify inclusion.

Since  $Z_{IB}$ , as defined, excludes both bulk water and water involved in hydrophobic hydration, any irrotationally bound water molecules must be due to the hydration of Na<sup>+</sup> or Cl<sup>−</sup>. Previous DRS investigations of a variety of salt solutions have produced a set of consistent and physically plausible  $Z_{IB}(\text{ion})$  values.<sup>14,16,27,43</sup> Analysis of these data, based on the (later confirmed<sup>43</sup>) assumption that  $Z_{IB}(\text{Cl}^-) = 0$ , gives the  $Z_{IB}(\text{Na}^+)$  values shown in Figure 7 (full line). Clearly, only for the most dilute sample is  $Z_{IB}(\text{NaBPh}_4) \approx Z_{IB}(\text{Na}^+) \approx 4.5$ . At  $c \geq 0.25$  M,  $Z_{IB}$  increases quickly to a plateau value of  $\sim 9$ . The discrepancy between the present  $Z_{IB}(\text{Na}^+)$  and those obtained previously<sup>14</sup> indicates that eq 14, which assumes the existence of bulk water whose behavior is not influenced by the electrolyte, does not give physically realistic results. Similarly, for Ph<sub>4</sub>PCl(aq) positive but scattered  $Z_{IB}$  values (not shown) are obtained, whereas the general consensus based on many types of measurement<sup>43,64</sup> is that  $Z_{IB}(\text{Cl}^-) \approx 0$ . Thus it appears that, except perhaps for very dilute NaBPh<sub>4</sub> solutions, the water molecules associated with relaxation processes 3 and 4 do not behave like normal bulk water but rather are significantly influenced by the electrolyte.

The apparent bulk-water concentration of eq 10 can be expressed as  $c_s^{app} = c_s g_K(c)/g_K(0)$ , where  $c_s$  is the true bulk-

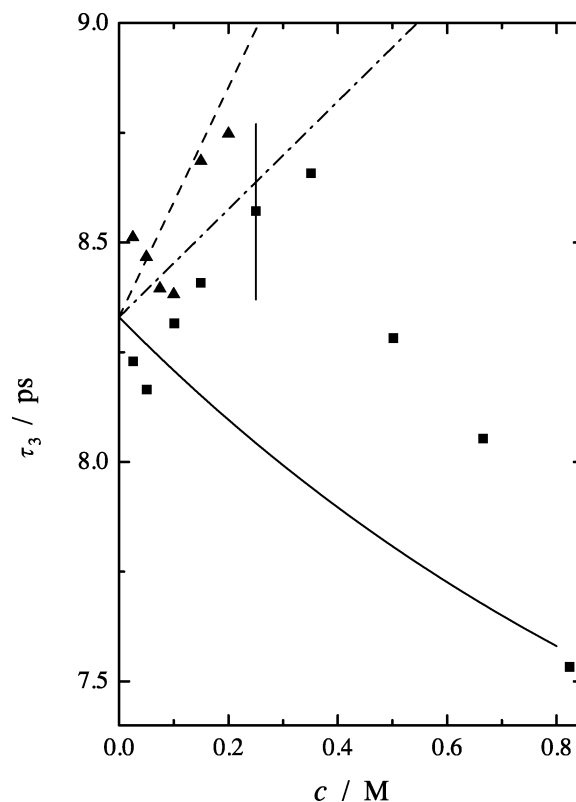


**Figure 8.** Concentration dependence of the bulk-water relaxation time  $\tau_3$  for NaBPh<sub>4</sub>(aq) (■, error bar at  $c = 0.25$  M given as an example) and Ph<sub>4</sub>PCl(aq) (▲) at 25 °C. Values for NaCl<sup>52</sup> (solid line), Me<sub>4</sub>NBr<sup>43</sup> (dash-dotted line) and higher tetraalkylammonium halides<sup>43</sup> (dashed line) are given for a comparison.

water concentration and  $g_K(c)/g_K(0)$  is the ratio of the Kirkwood factors of the solution and the pure solvent.<sup>30</sup> The apparent increase of  $Z_{IB}$  results from the significant decrease of  $g_K(c)$  ( $\sim 2.2$  at 0.8M) from the pure water value  $g_K(0) = 2.68$  (Figure 7). In other words, increasing solute concentration induces a gradual breakdown of the bulk-water structure which, in the pure state, is characterized by a strong parallel alignment of dipole vectors as a consequence of the flickering but percolating H-bond network with a locally-tetrahedral structure.<sup>48,51</sup> The breakdown starts at low concentrations but becomes more pronounced at  $c \gtrsim 0.35$  M, which corresponds to an average ionic distance  $l \lesssim 14 \text{ \AA} \approx 2(r_{\text{BPh}_4^-} + 2r_{\text{H}_2\text{O}})$ .

The relaxation time of the major bulk solvent process,  $\tau_3$ , is shown as a function of electrolyte concentration in Figure 8. For NaBPh<sub>4</sub>(aq), although the uncertainties are large,  $\tau_3$  appears to increase up to  $c \approx 0.35$  M and then decreases. The data for Ph<sub>4</sub>PCl(aq), which was only investigated at  $c \leq 0.20$  M, were similar.

The behaviour of  $\tau_3$  at low concentrations of NaBPh<sub>4</sub> and Ph<sub>4</sub>PCl is very similar to that observed for bulk water in the presence of the hydrophobic and structure-making tetraalkylammonium halides (Figure 8).<sup>43</sup> On the other hand, for NaCl (Figure 8) and other sodium salts containing typical inorganic structure-breaking anions<sup>27,52</sup> (not shown)  $\tau_3$  decreases continually with increasing electrolyte concentration. Thus at  $c \lesssim 0.35$  M, both NaBPh<sub>4</sub> and Ph<sub>4</sub>PCl stiffen the hydrogen-bond network even beyond the first hydration shell. At the same time this network is transformed from the structure of pure water to one where the overall parallel alignment of the water dipoles is reduced (see the above discussion of  $Z_{IB}$ ). This suggests that at low concentrations of a hydrophobic solute most of the long-range connectivity of the H<sub>2</sub>O molecules in a locally-tetrahedral



environment is still maintained in the newly formed bulk-water structure, possibly as water molecules bridging the hydrated ions. Only when more than one third of the total volume of the solution is occupied by the hydrated ions ( $c \geq 0.35$  M,  $l \leq 14$  Å) does the long-range structure collapse. This should lead to an increase in the number of dangling H-bonds and thus to a reduced activation energy<sup>20,43</sup> and a decrease of the dielectric relaxation time  $\tau_3$ .

Thus, on balance, the present DRS data and previous literature studies indicate that both  $\text{Ph}_4\text{P}^+$  and  $\text{BPh}_4^-$  are structure makers in dilute aqueous solution. However, they become structure breakers at higher concentrations when their volume fraction exceeds the threshold necessary for the maintenance of the H-bond network of water.

Most importantly, the present results show that the effects of both  $\text{Ph}_4\text{P}^+$  and  $\text{BPh}_4^-$  on water structure are very similar. This finding provides indirect support for the use of the reference electrolyte assumption based on  $\text{Ph}_4\text{PBPh}_4$ . Similar findings would be expected for  $\text{Ph}_4\text{AsBPh}_4$ .

**Acknowledgment.** The authors thank Dr. Ting Chen for measuring the VNA spectra of  $\text{NaBPh}_4(\text{aq})$ , and the Deutsche Forschungsgemeinschaft for a Mercator visiting professorship to GH and financial support to WW.

## References and Notes

- (1) Marcus, Y. *Ion Solvation*; Wiley: Chichester, 1985.
- (2) Popovych, O.; Tomkins, R. P. T. *Nonaqueous Solution Chemistry*; Wiley-Interscience: New York, 1981.
- (3) Kalidas, C.; Hefter, G.; Marcus, Y. *Chem. Rev.* **2000**, *100*, 819.
- (4) Hefter, G.; Marcus, Y.; Waghorne, W. E. *Chem. Rev.* **2002**, *102*, 2773.
- (5) Marcus, Y.; Hefter, G. *Chem. Rev.* **2004**, *104*, 3405.
- (6) Barthel, J. M. G.; Krienke, H.; Kunz, W. *Physical Chemistry of Electrolyte Solutions*; Steinkopff/Springer: Darmstadt/New York, 1998.
- (7) Conway, B. E. In *Modern Aspects of Electrochemistry*; Conway, B. E., White, R. E., Eds.; Kluwer Academic/Plenum: New York, 2002; Vol. 35.
- (8) Farmer, R. M.; Sasaki, Y.; Popov, A. I. *Austral. J. Chem.* **1983**, *36*, 1785.
- (9) Böttcher, C. J. F.; Bordewijk, P. *Theory of Electric Polarization*, 2nd ed.; Elsevier: Amsterdam, 1978; Vol. 2.
- (10) Scaife, B. K. P. *Principles of Dielectrics*; Clarendon: Oxford, 1989.
- (11) Barthel, J.; Buchner, R.; Eberspächer, P.-N.; Münsterer, M.; Stauber, J.; Wurm, B. *J. Mol. Liq.* **1998**, *78*, 83.
- (12) Buchner, R.; Barthel, J. *Annu. Rep. Prog. Chem. C* **2001**, *97*, 349.
- (13) Buchner, R. *Dielectric Spectroscopy of Solutions*. In *Novel Approaches to the Structure and Dynamics of Liquids: Experiments, Theories and Simulations*; Samios, J., Durov, V. A., Eds.; NATO Science Ser. II: Mathematics, Physics and Chemistry; Kluwer: Dordrecht, 2004; Vol. 133, pp 265-288.
- (14) Buchner, R.; Hefter, G. T.; May, P. M. *J. Phys. Chem. A* **1999**, *103*, 1.
- (15) Barthel, J.; Bachhuber, K.; Buchner, R.; Hetzenauer, H.; Kleebauer, M. *Ber. Bunsenges. Phys. Chem.* **1991**, *95*, 853.
- (16) Buchner, R.; Hefter, G.; May, P. M.; Sipos, P. *J. Phys. Chem. B* **1999**, *103*, 11186.
- (17) Barthel, J.; Popp, H. *J. Chem. Inf. Comput. Sci.* **1991**, *31*, 107. ELECTROLYTE DATA Regensburg is a subset of the database DETHERM (distributor: STN, Karlsruhe, Germany).
- (18) Havriliak, S.; Negami, S. *J. Polym. Sci. C* **1966**, *14*, 99.
- (19) Barthel, J.; Buchner, R.; Münsterer, M. *Electrolyte Data Collection, Part 2: Dielectric Properties of Water and Aqueous Electrolyte Solutions*; In Kreysa, G. (ed.), *Chemistry Data Series*; DEHEMA: Frankfurt am Main, 1995; Vol. 12.
- (20) Buchner, R.; Barthel, J.; Stauber, J. *Chem. Phys. Lett.* **1999**, *306*, 57.
- (21) Hölzl, C.; Schrödle, S.; Barthel, J.; Buchner, R. in preparation.
- (22) Rønne, C.; Thrane, L.; Åstrand, P.-O.; Wallqvist, A.; Mikkelsen, K. V.; Keiding, S. R. *J. Chem. Phys.* **1997**, *107*, 5319.
- (23) Kaatze, U. *J. Solution Chem.* **1997**, *26*, 1049.
- (24) Fukasawa, T.; Sato, T.; Watanabe, J.; Hama, Y.; Kunz, W.; Buchner, R. *Phys. Rev. Lett.* **2005**, *95*, 197802.
- (25) Sato, T.; Fukasawa, T.; Kunz, W.; Buchner, R. in preparation.
- (26) Zelsmann, H. R. *J. Mol. Struct.* **1995**, *350*, 95.
- (27) Wachter, W.; Kunz, W.; Buchner, R.; Hefter, G. *J. Phys. Chem. A* **2005**, *109*, 8675.
- (28) Subramanian, S.; Ahluwalia, J. C. *J. Phys. Chem.* **1968**, *72*, 2525.
- (29) Barthel, J.; Hetzenauer, H.; Buchner, R. *Ber. Bunsenges. Phys. Chem.* **1992**, *96*, 1424.
- (30) Buchner, R.; Capewell, S. G.; Hefter, G.; May, P. M. *J. Phys. Chem. B* **1999**, *103*, 1185.
- (31) *Quantities, Units and Symbols in Physical Chemistry*; 2nd ed.; Mills, I., Cvitaš, T., Homann, K., Kallay, N., Kuchitsu, K., Eds.; Blackwell: Oxford, 1993.
- (32) Zemaitis, J. F., Jr.; Clark, D. M.; Rafal, M.; Scrivner, N. C. *Handbook of Aqueous Electrolyte Thermodynamics: Theory and Application*; American Institute of Chemical Engineers: New York, 1986.
- (33) Robinson, R. A.; Stokes, R. H. *Electrolyte Solutions*; 2nd ed.; Butterworths: London, 1970.
- (34) Schiavo, S.; Fuoss, R. M.; Marrosu, G. *J. Solution Chem.* **1980**, *9*, 563.
- (35) Buchner, R.; Chen, T.; Hefter, G. *J. Phys. Chem. B* **2004**, *108*, 2365.
- (36) Rudolph, W. W.; Irmer, G.; Hefter, G. T. *Phys. Chem. Chem. Phys.* **2003**, *5*, 5253.
- (37) Hefter, G. T. *Pure Appl. Chem.*, in press.
- (38) Covington, A. K.; Tait, M. J. *Electrochim. Acta* **1967**, *12*, 123.
- (39) Buchner, R.; Samani, F.; May, P. M.; Sturm, P.; Hefter, G. *ChemPhysChem* **2003**, *4*, 373.
- (40) Buchner, R.; Barthel, J. *J. Mol. Liq.* **1995**, *63*, 55.
- (41) Strehlow, H.; Knoche, W. *Fundamentals of Chemical Relaxation*; Verlag Chemie: Weinheim, 1977.
- (42) Cavell, E. A. S.; Knight, P. C.; Sheikh, M. A. *J. Chem. Soc., Faraday Trans.* **1971**, *67*, 2225.
- (43) Buchner, R.; Hölzl, C.; Stauber, J.; Barthel, J. *Phys. Chem. Chem. Phys.* **2002**, *4*, 2169.
- (44) Baar, C.; Buchner, R.; Kunz, W. *J. Phys. Chem. B* **2001**, *105*, 2906.
- (45) Tromans, A.; May, P. M.; Hefter, G.; Sato, T.; Buchner, R. *J. Phys. Chem. B* **2004**, *108*, 13789.
- (46) Sunder, S.; Chawla, B.; Ahluwalia, J. C. *J. Phys. Chem.* **1974**, *78*, 738.
- (47) M'Halla, J.; M'Halla, S. *J. Chim. Phys.* **1999**, *96*, 1450.
- (48) Ohmine, I.; Tanaka, H. *Chem. Rev.* **1993**, *93*, 2545.
- (49) Kaatze, U.; Behrends, R.; Pottel, R. *J. Non-Cryst. Solids* **2002**, *305*, 19.
- (50) Sato, T.; Buchner, R. *J. Chem. Phys.* **2003**, *119*, 10789.
- (51) Stanley, H. E.; Teixeira, J. *J. Chem. Phys.* **1980**, *73*, 3404.
- (52) Capewell, S. G.; Buchner, R.; Hefter, G.; May, P. M. *Phys. Chem. Chem. Phys.* **1999**, *1*, 1933.
- (53) Marcus, Y. *Ion Properties*; Dekker: New York, 1997.
- (54) Gibbs, H. J.; Fleming, P. D., III; Porosoff, H., In: *The Physical Chemistry of Aqueous Systems*; Kay, R. L., Ed.; Plenum: New York, 1973.
- (55) Bockris, J. O' M.; Saluja, P. P. S. *J. Phys. Chem.* **1972**, *76*, 2140.
- (56) Yoshida, K.; Ibuki, K.; Ueno, M. *J. Solution Chem.* **1996**, *25*, 435.
- (57) Schiavo, S.; Marrosu, G. *Z. Phys. Chem. NF* **1977**, *105*, 157.
- (58) Millero, F. J. *J. Chem. Eng. Data* **1970**, *15*, 562.
- (59) Hepler, L. G. *Can. J. Chem.* **1969**, *47*, 4613.
- (60) Jolicœur, C.; The, N. D.; Cabana, A. *Can. J. Chem.* **1971**, *49*, 2008.
- (61) Stangret, J.; Kamieńska-Piotrowicz, E. *J. Chem. Soc., Faraday Trans.* **1997**, *93*, 3463.
- (62) Coetzee, J. F.; Sharpe, W. R. *J. Phys. Chem.* **1971**, *75*, 3141.
- (63) Marcus, Y. *J. Solution Chem.* **1994**, *23*, 831.
- (64) Ohtaki, H.; Radnai, T. *Chem. Rev.* **1993**, *93*, 1157.